Biochemical Pharmacology 82 (2011) 681–691

Contents lists available at ScienceDirect

Biochemical Pharmacology

journal homepage: www.elsevier.com/locate/biochempharm

Drug metabolism by CYP2C8.3 is determined by substrate dependent interactions with cytochrome P450 reductase and cytochrome b5☆

Rüdiger Kaspera [a], Suresh B. Naraharisetti [a,1], Eric A. Evangelista [a], Kristin D. Marciante [b], Bruce M. Psaty [b,c,d,e], Rheem A. Totah [a,*]

[a] Department of Medicinal Chemistry, Box 357610, University of Washington, Seattle, WA 98195-7610, USA
[b] Cardiovascular Health Research Unit, Department of Medicine, University of Washington, Seattle, WA, USA
[c] Department of Epidemiology, University of Washington, Seattle, WA, USA
[d] Department of Health Services, University of Washington, Seattle, WA, USA
[e] Group Health Research Institute, Group Health Cooperative, Seattle, WA, USA

ARTICLE INFO

Article history:
Received 29 April 2011
Accepted 16 June 2011
Available online 24 June 2011

Keywords:
Paclitaxel
Amodiaquine
Rosiglitazone
Cerivastatin
Pharmacogenetics
Ligand binding

ABSTRACT

Genetic polymorphisms in *CYP2C8* can influence the metabolism of important therapeutic agents and cause interindividual variation in drug response and toxicity. The significance of the variant *CYP2C8*3* has been controversial with reports of higher *in vivo* but lower *in vitro* activity compared to *CYP2C8*1*. In this study, the contribution of the redox partners cytochrome P450 reductase (CPR) and cytochrome b5 to the substrate dependent activity of CYP2C8.3 (R139K, K399R) was investigated in human liver microsomes (HLMs) and *Escherichia coli* expressed recombinant CYP2C8 proteins using amodiaquine, paclitaxel, rosiglitazone and cerivastatin as probe substrates. For recombinant CYP2C8.3, clearance values were two- to five-fold higher compared to CYP2C8.1. CYP2C8.3's higher k_{cat} seems to be dominated by a higher, but substrate specific affinity, towards cytochrome b5 and CPR (K_D and $K_{m,red}$) which resulted in increased reaction coupling. A stronger binding affinity of ligands to CYP2C8.3, based on a two site binding model, in conjunction with a five fold increase in amplitude of heme spin change during binding of ligands and redox partners could potentially contribute to a higher k_{cat}. In HLMs, carriers of the *CYP2C8*1/*3* genotype were as active as *CYP2C8*1/*1* towards the CYP2C8 specific reaction amodiaquine *N*-deethylation. Large excess of cytochrome b5 compared to CYP2C8 in recombinant systems and HLMs inhibited metabolic clearance, diminishing the difference in k_{cat} between the two enzymes, and may provide an explanation for the discrepancy to *in vivo* data. *In silico* studies illustrate the genetic differences between wild type and variant on the molecular level.

1. Introduction

Cytochrome P450 2C8 (CYP2C8) accounts for 7% of the total hepatic CYP content [1,2] and is estimated to be involved in the metabolism of at least 5% of drugs cleared by phase I oxidative processes [3]. CYP2C8 is predominantly involved in the drug metabolism of amodiaquine (AQ), amiodarone, cerivastatin (CER), montelukast, paclitaxel (PAC), repaglinide, rosiglitazone (RG), and troglitazone [3,4]. CYP2C8 also contributes to the metabolism of endogenous substrates such as the epoxidation of arachidonic acid [5] and hydroxylation of *all trans* retinoic acid [6]. From the at least 17 genetic variants described for *CYP2C8* (http://www.cypalleles.ki.se/cyp2c8.htm), *CYP2C8*3* is the most common in Caucasians (allele frequency of up to 0.15) [7] but seems to be absent in African Americans and attracted particular attention vis-à-vis its effect on drug metabolism.

*CYP2C8*3* encodes a protein with two amino acid substitutions at R139K and K399R, which are highly linked (>95%) [8]. Reports investigating the effect of these mutations on the clearance of CYP2C8 substrates *in vivo* were recently reviewed [9]. The inheritance of one or more alleles of *CYP2C8*3* is correlated with an increased clearance *in vivo* but overall, studies failed to consistently connect the *CYP2C8*3* allele to alteration in pharmacokinetics (see [9] and citations within). Discrepancies were mostly explained by other contributing CYP enzymes, diverse study design and other metabolic pathways depending on substrate.

☆ This work was supported by Grant National Institutes of Health RO1 HL-078888 and National Institute of General Medical Sciences GM P01 32165.

Abbreviations: CYP, cytochrome P450; CPR, cytochrome P450 reductase; CER, cerivastatin; AQ, amodiaquine; PAC, paclitaxel; RG, rosiglitazone; DEAQ, *N*-de ethyl amodiaquine; DLPC, L-α-dilauryl-sn-glycero-3-phosphocholine; HLMs, human liver microsomes; SIR EI^+, selective ionization reaction positive ionization; MRM EI^+, multiple reaction mode positive ionization.

* Corresponding author. Tel.: +1 206 543 9481; fax: +1 206 685 3252.
E-mail address: rtotah@uw.edu (R.A. Totah).
[1] Current address: Office of Clinical Pharmacology, Center for Drug Evaluation and Research, U.S. Food and Drug Administration, Silver Spring, MD, USA.

0006-2952/$ – see front matter © 2011 Elsevier Inc. All rights reserved.
doi:10.1016/j.bcp.2011.06.027

Reports investigating the metabolic activity of the expressed variant protein CYP2C8.3 *in vitro* have also been controversial. Several investigators contradict *in vivo* findings with lower metabolic rates for AQ *N*-de-ethylation [10,11], a slightly lower rate of PAC 6α-hydroxylation [7,12] and arachidonic acid epoxidation [13] *in vitro*. Other studies report also slightly higher metabolic rates for PAC and 13-*cis*-retinoic acid in partially purified recombinant CYP2C8.3 [14]. Each study used a different expression system such as *E. coli*, or partially purified *E. coli* membrane systems, without the addition cytochrome b5 [7,14,15], yeast [11] or HepG2 cells [12]. In contrast, recombinant CYP2C8.3 reconstituted with CPR and cytochrome b5 demonstrated a higher activity towards CER [8], a finding that is consistent with the above mentioned *in vivo* data. Interestingly, both amino acid mutations (R139K and K399R) in the corresponding CYP2C8.3 protein are located on the proximal site of the heme in the binding region of cytochrome b5 and CPR [16] and may suggest an involvement of the redox-partners in the variable activity of CYP2C8. The activation of CYP enzymes by cytochrome b5 is well established [17] for CYP3A4 [18], CYP2B4 and variants [19], CYP2A6 [20], CYP2C9 [21] and CYP2C19 [22]. Further, cytochrome b5 is also reported to decrease reaction uncoupling [23] and increase k_{cat}.

This investigation aimed to assess the effect of cytochrome b5 and CPR on a particular CYP2C8 genetic variant of clinical significance. For this purpose, metabolic activities of genotypes *CYP2C8*1* and *CYP2C8*3* were tested using a range of substrates *in vitro* in HLMs derived from individual human donor livers with pre-determined *CYP2C8* genotypes, CYP2C8 protein, CPR and cytochrome b5 content. These studies revealed either a slightly higher or equal metabolic activity of the *CYP2C8*3* genotype which is consistent with reported data for other drugs such as repaglinide *in vivo* [24]. Interestingly CYP2C8 activity was inversely associated with CYP b5 content. These data, however, do not align with published data for recombinantly expressed CYP2C8.3 protein. Consequently, CYP2C8.1 and CYP2C8.3 were engineered and expressed and kinetically evaluated towards the metabolic activity of probe substrates, ligand binding and affinity towards cytochrome b5 and CPR. The interaction of CYP2C8.3 protein with its redox partners was further rationalized *in silico* to address the structural differences caused by these two point mutations.

2. Materials and methods

2.1. Materials

All chemicals including terfenadine and chloroquine were purchased from Sigma-Aldrich (St. Louis, MO, USA), unless otherwise stated, and used without further purification. CER sodium salt ((3R,5S,6E)-7-[4-(4-Fluorophenyl)-5-(methoxymethyl)-2,6-bis(1-methylethyl)-3-pyridinyl]-3,5-dihydroxy-6-heptenoic Acid Sodium Salt), hydroxy CER (M23, 6-[(1S)-2-hydroxy-1-methylethyl]-metabolite), desmethyl CER (M1, 5-(hydroxyl-methyl)-metabolite), RG, *N*-desmethyl RG, and 5-hydroxy RG were purchased from Toronto Research Chemicals (North York, ON, CA). Fluvastatin was a gift from em. Professor W. Trager (University of Washington). 6-Hydroxy PAC and DEAQ were purchased from Santa Cruz Chemicals (Santa Cruz, CA). Protein test kit was purchased from Pierce Biotechnology (Rockford, IL). Acetonitrile, methanol, water, zinc sulfate, ammonium formate and formic acid were purchased from Fisher Scientific (Pittsburgh, PA, USA). L-α-Dilauryl-sn-glycero-3-phosphocholine (DLPC) was from Avanti Polar Lipids Inc., (Alabaster, AL, USA). Human liver samples were obtained from the University of Washington School of Pharmacy Human Tissue Bank (Seattle, WA) (*24, 25*).

2.2. Expression of cytochrome P450 reductase, cytochrome b5 and CYP2C8.1 (wild type) and CYP2C8.3

Rat cytochrome P450 reductase and cytochrome b5 were expressed using previously established protocols [25,26]. The two base pair changes rs11572080 and rs10509681 for genotype *CYP2C8*3* were introduced into CYP2C8 (wild type) using site directed mutagenesis and the wild type and variant were expressed as previously described [13]. P450-CO difference spectra, gel electrophoresis, pyridine hemochromogen analysis and Lowry protein determination assay were used to evaluate CYP-enzyme quality and quantity [27,28]. Time of flight mass spectrometry (Waters Micromass High-Definition MS System, Quadrupole/Triwave™/Orthogonal Acceleration Time-of-Flight Tandem Hybrid Mass Spectrometer QToa – TOF MS/IMS/MS) was used to characterize the molecular mass of CYP2C8 proteins using the separation method of Cheesman et al. [29]. Mass determination resulted in a MW of 56,815 ± 13 for CYP2C8.1 and 56,837 ± 10 for CYP2C8.3 (calc. MW for both CYP2C8.1 and CYP2C8.3 protein 56835.77).

2.3. Characterization of human liver microsomes

Samples of human liver ($n = 56$) from Caucasian donors were obtained from the University of Washington School of Pharmacy Human Tissue Bank (Seattle, WA) according to previously published protocols [30]. Protein concentrations were determined by the method of Lowry et al. [31]. Genotype of *CYP2C8*3* and corresponding CYP2C8 protein content were previously determined [32].

2.4. In vitro assays for recombinant CYP2C8 and human liver microsomes

DLPC micelles (2.5 mM) were prepared by repeated sonication and supplemented in the order of CYP2C8, cytochrome P450 reductase, and cytochrome b5 in the ratio 160:1:2:1 [33] – the ratio CYP:DLPC was constant for all kinetic evaluations. The mixture was incubated on ice for 20 min and diluted with potassium phosphate buffer (100 mM KPi, pH 7.4) to reach final assay concentration of 50 pmol mL^{-1} for AQ, CER, and RG, and for PAC metabolism. For enzyme kinetics, 0.2 mg mL^{-1} of human liver microsomes or 10 pmol P450 mL^{-1} of recombinant CYP2C8 were used as final concentrations in the assay mixture.

AQ and RG metabolism: Assay mixtures were supplemented with substrate at final concentrations 0.1–200 μM (for kinetics), pre-incubated for 5 min at 37 °C in a shaking water bath. Reactions were initiated by adding 10 μL of 10 mM NADPH to 90 μL assay mixture for a total volume of 100 μL. The AQ incubations were quenched with 10 μL 10% trichloracetic acid after 5 min; the assay for the RG metabolism was terminated after 5 min incubation by adding 10 μL of 15% zinc sulfate. Subsequently, internal standard (10 μL to achieve a final concentration of 0.26 μM chloroquine for AQ and 0.5 μM terfenadine for RG) was added. Samples were immediately vortexed, centrifuged at 10,000 × *g* for 10 min at room temperature and 10 μL (15 μL for RG) of supernatant was injected into LC–MS for analysis. DEAQ, *p*-hydroxy RG (PHRG), and demethyl RG (DMRG) were quantified by using a standard calibration curve ranging from 0.005 to 2.5 μM.

PAC metabolism: 450 μL of 100 mM KPi buffer with PAC (concentration range 0.1–100 μM) and reconstituted CYP enzyme with above mentioned concentrations were pre-incubated for 5 min at 37 °C and the assay was initiated by adding 50 μL of 10 mM NADPH. Reactions were quenched after 30 min by adding 2 mL ice-cold ethyl acetate containing internal standard (25 nM 10-deacetyl baccatin III), extracted and the organic phase removed. Extraction was repeated twice with 2 mL ethyl acetate; the organic phases were pooled for a total of 6 mL, evaporated to

dryness under a nitrogen flow and the residue re-suspended in 50 μL methanol–water mixture (50:50) of which 25 μL was used for analysis by LC–MS. The calibration curve for 6α-hydroxy paclitaxel ranged from 0.05 to 1 μM.

CER metabolism: The assay was performed as previously described [8].

For each substrate, k_{cat}/K_m determination was performed (in duplicate) under linear conditions with respect to time and protein. Heat-denatured enzymes or HLMs and incubation mixtures without NADPH served as negative controls.

2.5. Assays for measuring CYP2C8:CPR:cytochrome b5 interactions and NADPH depletion

To investigate whether the ionic strength of assay buffer influences activity of reconstituted CYP2C8 towards DEAQ formation, the ionic strength of buffer was gradually increased by diluting the reconstituted enzymes in HEPES with concentrations from 50–1000 mM according to Kelley et al. [34]. Subsequently, to assess the concentration dependency of cytochrome b5 and CPR on CYP2C8 activity, the content of cytochrome b5 was increased from the ratio of 0:1 to 10:1 (b5:CYP2C8) during reconstitution while CYP enzyme and CPR concentration were kept constant (1:2 ratio) as mentioned under *in vitro* assays. The experiment was repeated and CPR concentration gradually increased using the same ratios, while keeping CYP enzyme and cytochrome b5 concentration at a constant ratio of 1:1. The CYP2C8 activity was measured at 10 μM substrate concentration as mentioned above, as some substrates showed substrate inhibition kinetics. NADPH depletion was measured as previously described [23] following the linear decrease absorption at 340 nm over 5 min at 0.1 mM NADPH, 5 μM AQ and 50 pmol mL^{-1} CYP2C8.1 or CYP2C8.3 reconstituted with CPR and cytochrome b5 in a 1:2:1 ratio, respectively. After 3 min incubation at 37 °C, an aliquot was sampled from the cuvette to quantify DEAQ formation by LC–MS. Reaction coupling was expressed as percent of mols DEAQ formed per mols NADPH depleted.

2.6. Analysis of metabolite formation

AQ and RG metabolites were quantified using HPLC in tandem with an electrospray-mass spectrometer (HP1100 liquid chromatograph, a G1367A auto sampler, a G1312A binary pump, a G1322A degasser and a G1948A mass selective detector, all components Hewlett–Packard, Palo Alto, CA). The HPLC/MS system was connected to ChemStation software version 10.02 (Hewlett–Packard) which was used for data analysis. AQ, chloroquine (CQ: internal standard) and DEAQ were co-eluted on an Agilent Zorbax XDB C8-column (2.1 μm, 5 cm, flow 0.35 mL min^{-1}), using a gradient elution (mobile phases A: 2.0 mM ammonium formate with 0.1% formic acid in water and B: 2.0 mM ammonium formate with 0.1% formic acid in acetonitrile, elution profile: B: 0 min 5%, 1.5 min 40%, 1.51 min 90%, 4 min 90%, 4.1 min 90%, 5 min 5%). Compounds were detected by SIR EI^+ $[M+1]^+$ using *m/z* 356 (AQ), 328 (DEAQ) and 320 (CQ) using a fragmentor voltage of 75 (AQ), 100 (DEAQ) and 125 V (CQ), a capillary voltage of 5000 V, drying gas temperature 350 °C, drying gas flow 10 L min^{-1} and nebulizer pressure 25 psig.

RG, desmethyl RG (DMRG), *para*-hydroxy RG (PHRG) and terfenadine (TER, internal standard) were separated on the same column using the mobile phase A: 10 mM ammonium acetate pH 8.0 in water and B: methanol, flow rate of 0.3 mL min^{-1} and a gradient elution profile (% B: 0 min 20%, 0.5 min 20%, 1 min 80%, 2 min 100%, 4 min 100%, 4.1 min 20%, 5 min 20%). Detection was performed in SIR EI^+, $[M+1]^+$ with *m/z* 358 (RG), 344 (DMRG), 374 (PHRG) and 472 (TER) using a fragmentor voltage of 150 V for RG and 100 V for DMRG, PHRG and TER, a capillary voltage of 5000 V, a drying gas temperature of 350 °C, a drying gas flow of 10 L min^{-1} and a nebulizer pressure of 25 psig.

POH, PAC and 10-deacetyl baccatin III (DAB, int. standard) were separated on a Waters ACQUITY Ultra Performance LC™ system using a Thermo Hypersil Gold C8 column (2.1 × 50, flow 0.3 mL min^{-1}) and a gradient elution program (eluents A: 10 mM ammonium acetate pH 5.5, and B: methanol, elution profile: B: 0 min 35%, 1 min 35%, 2 min 100%, 3 min 100%, 3.1 min 35%, 4 min 35%). Compounds were detected in MRM EI^+ using the ion transitions 877.06 $[M+Na+1]^+ > 308.20$ (PAC), 892.97 $[M+Na+1]^+ > 308.15$ (POH), 562.39 $[M+NH_4+1]^+ > 105.41$ (DAB), on a Waters Micromass Quattro Premier XE (connected to MassLynx 4.1). For ionization and fragmentation, a capillary voltage of 3.5 kV was used with the following parameters for each compound, for PAC cone voltage (CV) 10 V, collision energy (CE) 35 V; for POH: CV 15 V, CE 35 V; and for DAB: CV 20 V, CE 35 V.

2.7. Quantitation of cytochrome b5 and cytochrome P450 reductase

For human liver microsomes, NADPH-cytochrome c reduction activities were determined as described previously [35]. P450 reductase concentrations were calculated assuming a specific activity of 3.0 μmol of cytochrome c reduced per minute per nanomole of reductase, based on published data for purified human and rabbit reductase preparations [15]. The concentration of cytochrome b5 was calculated spectrally following published methods [28,36]. Additional values were extracted from Huang et al. [36].

2.8. Sequence alignment and structural evaluation

Sequences were taken from NCBI website with the following accession numbers: CYP2C8 (NP_000761.3), CYP2C9 (NP_000762.2), CYP2C18 (NP_000763.1), CYP2C19 (NP_000760.1), CYP1A2 (AAH67427), CYP2A6 (NP_000753), CYP2B4 (P00178), CYP2B6 (NP_000758.1), CYP2D6 (NP_001020332.1), CYP2E1 (NP_000764.1), CYP2J2 (NP_000766.2), CYP3A4 (NP_059488.2), CYP4F12 (NP_076433.2), CYP101 (P00183.2), and CYP102 (P14779). Sequence alignment was performed using clustalW2 (EMBL-EBI) and the figure rendered in genedoc (version 2.7.000, 2006). Sequences are aligned in order of their phylogenetic distance to CYP2C8.

A homology model of CYP2C8.3 was generated using the Swiss model workspace using the CYP2C8.3 protein sequence to thread on the template structure 2NNI [37]. Electrostatic energy surfaces were calculated using Adaptive Poisson-Boltzmann Solver 1.2.1 [38]. Salt bridges were calculated in Visual Molecule Dynamics (VMD version 1.8.7) [39] with a 3.5 Å cut off value. Molecular distances were measured and structures visualized in PyMOL (PyMOL Molecular Graphics System, Version 1.3, Schrödinger, LLC).

2.9. Resting state, ligand and redox cofactor binding studies

Resting spin state of CYP2C8 was determined by Gaussian deconvolution of the absolute spectra into 360 nm (δ), 390 nm (high spin) and 417 (low spin) using OriginPro version 7.5 (OriginLab Corp., Northampton, MA). Ligand binding to the purified CYP2C8.1 and CYP2C8.3 protein was performed at 25 °C on a modernized Olis Aminco DW-2 (Olis Inc. Bogart, CA). 1% CHAPS in 100 mM phosphate buffer (KPi, pH 7.4), added to reference and sample cuvette with 2 μM purified CYP-enzyme added to the sample cuvette. 1 μL substrate or redox cofactor was added to sample and reference cuvette, and the full spectra from 350 to 700 nm recorded. Ligands were initially dissolved in methanol, except rosiglitazone (DMSO) and diluted out stepwise in phosphate buffer (50 mM, pH 7.4). A decrease at 420 nm was used for K_D calculations as using the absorbance difference at 646–570 nm led to similar results, but

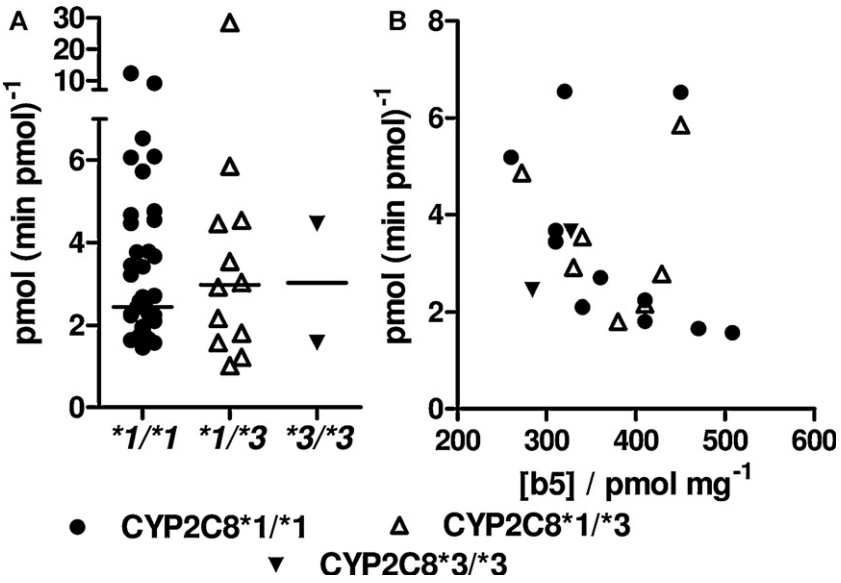

Fig. 1. (A) DEAQ formation (k_{cat}/K_m) from AQ normalized to CYP2C8 content (pmol mg^{-1}) and categorized by CYP2C8 genotypes of human liver microsomes ($P = 0.90$ for *CYP2C8*1/*1* compared to *CYP2C8*1/*3*) and (B) formation of DEAQ (k_{cat}/K_m) per CYP2C8 content displayed against cytochrome b5 content of each corresponding liver.

delivered less precision at 2 μM protein concentration. Difference spectra were calculated by subtracting measurements from the baseline (enzyme without addition of ligand). The binding data were fit using Graphpad Prism, and further evaluated using DynaFit 3.28.070 [40] using floating molar responses with different binding modes as described previously [41].

2.10. Statistical analysis

Apparent Michaelis–Menten constants K_m and k_{cat} were derived after nonlinear regression analysis of the kinetic data using a Michaelis–Menten, or substrate inhibition model where applicable (SigmaPlot 2004 windows version 9.0, Systat Software, Chicago, IL). Apparent kinetic constants for P450 reductase – CYP2C8 complex formation measured through CYP2C8 activity were calculated as $K_{m,red}$ values. Kinetic data is reported as the mean ± S.D. (computer generated). Statistical significance of median differences (Fig. 1) was assessed using Mann–Whitney test (Fig. 2) or two-tailed *t*-test (Tables 1–3, with $^{*}P < 0.05$, $^{**}P < 0.01$, $^{***}P < 0.001$) (GraphPad Prism version 5.02, GraphPad Software Inc., San Diego, CA).

3. Results

3.1. AQ and RG metabolism in human liver microsomes

DEAQ formation, specific for CYP2C8 mediated metabolism, was used to investigate metabolic activity of HLMs carrying the genotypes *CYP2C8*1/*1*, *CYP2C8*1/*3*, and *CYP2C8*3/*3* obtained from the University of Washington School of Pharmacy Human Tissue Bank (Seattle, Washington, USA) [42]. These HLMs were previously genotyped and the CYP2C8 protein content measured [32]. Metabolic activity was measured at 0.2, 2 and 20 μM (0.1K_m, K_m, and 10K_m respectively), a formation clearance (k_{cat}/K_m) was estimated and then normalized to CYP2C8 content [32]. Livers carrying the *CYP2C8*1/*1* genotype demonstrated a slightly lower clearance (k_{cat}/K_m) for AQ (not statistically significant) in comparison to *CYP2C8*1/*3* and *CYP2C8*3/*3* (Fig. 1A).

To investigate if cytochrome b5 and CPR might influence the activity of the CYP2C8 wild type and variant, cytochrome b5 and CPR protein content was measured in a subset of 20 livers (Fig. 1B). Cytochrome b5 concentrations ranged from 260 to 520 pmol mg^{-1} resulting in a ratio of cytochrome b5: CYP2C8 ranging from 5:1 to

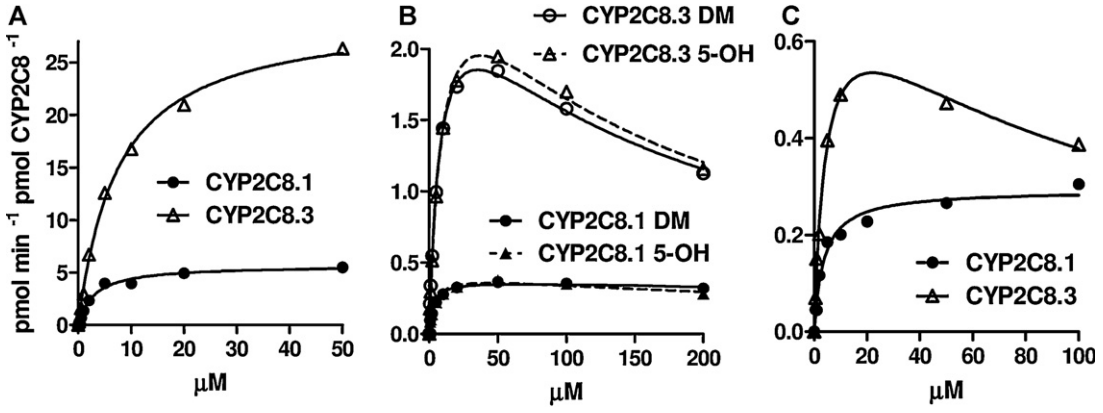

Fig. 2. Kinetic evaluation of (A) AQ *N*-de-ethylation, (B) RG *p*-hydroxyation (DM: desmethyl RG; 5-OH: *para*-hydroxy RG), and (C) PAC 6α-hydroxylation (at a ratio of CYP2C8:CPR:cytochrome b5 1:2:1 respectively).

Table 1
Kinetic constants of reconstituted CYP2C8.1 and CYP2C8.3 with different substrates.

	CYP2C8.1			CYP2C8.3		
	K_m (μM)	k_{cat} (nmol nmol P450^{-1} min^{-1})	Cl_{int} (μM^{-1} min^{-1})	K_m (μM)	k_{cat} (nmol nmol P450^{-1} min^{-1})	Cl_{int} (μM^{-1} min^{-1})
AQ	3.0 ± 0.4	5.7 ± 0.2	1.9	7.5 ± 0.5 (**)	29.8 ± 0.7 (***)	4.0
RG						
p-hydroxylation	4.0 ± 0.8	0.42 ± 0.03	0.11	10.2 ± 0.9 (*)	3.0 ± 0.1 (***)	0.29
N-de-methylation	2.9 ± 0.6	0.38 ± 0.02	0.13	8.0 ± 0.6 (*)	2.7 ± 0.1 (***)	0.33
PAC	3.7 ± 0.6	0.29 ± 0.01	0.11	4.7 ± 0.7 (-)	0.76 ± 0.06 (**)	0.16
CER[a]						
hydroxylation	23 ± 2	0.22 ± 0.01	0.0096	13 ± 2 (*)	0.61 ± 0.03 (**)	0.047
O-de-methylation	24 ± 3	0.57 ± 0.02	0.024	13 ± 2 (*)	1.47 ± 0.06 (**)	0.11

[a] Adapted from [8].

65:1 with most livers in the range of 5–10:1. CPR content displayed low interindividual variability ranging from a ratio of 36:1 to 56:1 to CYP2C8 content. The protein content of cytochrome b5 and CPR was consistent with previous reports [36,43]. An increase in cytochrome b5 content inversely correlated with k_{cat}/K_m for DEAQ formation per CYP2C8 content, (Fig. 1B), whereas no correlation was observed between metabolic activity and CPR content (data not shown).

3.2. Kinetic evaluation of CYP2C8 probe substrates in recombinant enzymes

Recombinant CYP2C8 reconstituted with CPR and cytochrome b5 in a ratio of 1:2:1 demonstrated Michaelis–Menten kinetics (Fig. 2 and Table 1). Kinetics for CER were adapted from earlier studies (*8*). The K_m values for PAC was similar for CYP2C8.3 and CYP2C8.1 but were two to three times higher for AQ and RG as representative basic compounds in comparison to CYP2C8.1 (Table 1). In contrast, K_m was lower for the acidic compound CER with CYP2C8.3 compared to CYP2C8.1. k_{cat} was remarkably higher (up to 7 times) in comparison to CYP2C8.1 across the board for all substrates tested. As a result, a 2-fold higher Cl_{int} (k_{cat}/K_m) for DEAQ formation, an up to 3-fold higher Cl_{int} for *p*-hydroxy (the specific CYP2C8 metabolite) and *N*-de-methyl RG, but only a 1.5 fold increase for PAC 6α-hydroxylation for CYP2C8.3 compared to CYP2C8.1 was observed.

In contrast to AQ, substrate inhibition kinetics were observed for the metabolism of RG (K_i = 150 μM) and PAC (K_i = 103 μM) only for CYP2C8.3, whereas substrate inhibition for CYP2C8.1 was negligible.

3.3. Interactions of redox partners with CYP2C8.1 and CYP2C8.3

As the most CYP2C8 specific probe reaction, DEAQ formation was chosen to determine the effect of the redox partners, cytochrome b5 and CPR, on the catalytic activity of CYP2C8 proteins. For this purpose and for an initial assessment, a stepwise increase of the salt concentration in the assay buffer was used to diminish electrostatic interactions between the protein complex in general, since the mutational changes between CYP2C8.1 and CYP2C8.3 affect two charged amino acid residues R139K and K399R located within the cytochrome b5 and CPR binding region [8,19]. The concentration of HEPES was increased in the assay buffer of reconstituted enzymes as HEPES has given the most gradual decrease of these interactions in comparison to bivalent salts [34]. The activity for CYP2C8.3 was more stable at higher buffer concentrations whereas CYP2C8.1 activity decreased at lower buffer concentrations (Fig. 3). To further investigate the effect of each redox partner separately on the activity of CYP2C8.1 and CYP2C8.3 substrates, the turnover of each of the four substrates was measured at varying ratios of cytochrome b5 to CYP2C8 in the reconstitution system while keeping the ratio CPR to CYP2C8 at 2:1 (Fig. 4, full kinetic profile displayed in Supplementary Material). Subsequently, the ratio of CPR to CYP2C8 protein was changed while keeping the ratio cytochrome b5 to CYP2C8 at 1:1 (Fig. 5).

Table 2
Apparent dissociation constants for CYP–CPR and CYP–cytochrome b5 interactions measured indirectly through activity for each probe reaction.

	P450–CPR	
Protein	CYP2C8.1	CYP2C8.3
Substrate	$K_{m,red}$ (nM)	$K_{m,red}$ (nM)
AQ[a]	81 ± 12	33 ± 5 (*)
CER[b]	105 ± 10	90 ± 10 (-)
PAC[c]	35 ± 10	5.5 ± 1.5 (*)
RG[d]	86.5 ± 19	19 ± 4 (*)

[a] DEAQ-formation.
[b] CER hydroxylation (M23-formation).
[c] PAC 6α-hydroxylation.
[d] RG *p*-hydroxylation.

3.3.1. Effect of cytochrome b5

In absence of cytochrome b5 in the reconstitution system, CYP2C8.3 exhibited higher activity compared to CYP2C8.1 for AQ and CER, whereas for RG and PAC, CYP2C8.3 was less active (Fig. 4). Increasing the ratio of cytochrome b5 to CYP2C8 unmasked the difference between variant and wild type protein activities with a maximum difference at a ratio of 1:1 (CYP2C8:CYP b5) for all substrates (up to 6-fold for AQ). Interestingly, an excess of cytochrome b5 of 1:10 ratio inhibited the activity of both wild type and variant. CYP2C8.3 still displayed higher activity for all substrates (DEAQ formation remained six fold higher with increasing cytochrome b5 ratio), with the exception of CER for which increasing cytochrome b5 concentrations obscured the higher activity of CYP2C8.3. Further, cytochrome b5 inhibited CYP-activity in a substrate dependent manner. Whereas strong

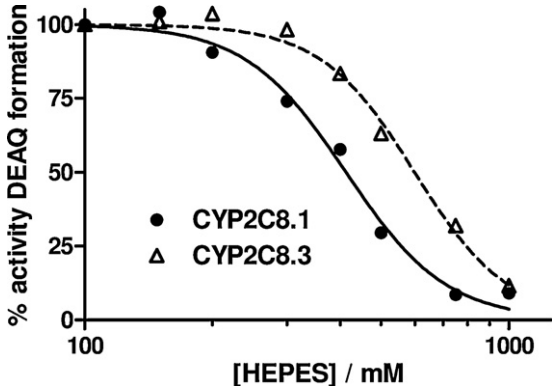

Fig. 3. Percent activity of AQ *N*-de-ethylation for recombinant CYP2C8.1 and CYP2C8.3 at the ratio of CYP:cytochrome b5:CPR of 1:2:1 at increasing HEPES concentrations (initial 100% activity measured at 100 mM HEPES buffer).

Table 3
Equilibrium binding constants of substrates binding to CYP2C8.1 and CYP2C8.3 (according to a two site binding model with low K_D and high K_D).

	K_D		% change in B_{max}[a]
Protein	CYP2C8.1	CYP2C8.3	
Substrate	(μM)	(μM)	
AQ	0.006 ± 0.001; 3.0 ± 0.9	0.003 ± 0.001; 0.15 ± 0.07	+3; −8
CER	0.4 ± 0.2; 3.9 ± 9.3	0.16 ± 0.02; 8.2 ± 2.2	+45; +533
PAC	0.42 ± 0.06; 24.4 ± 5.2	0.46 ± 0.12; 11.7 ± 7.6	+79; −14
RG	0.002 ± 0.001; 0.22 ± 0.08	<0.001; 0.11 ± 0.08	+5; +258
	(nM)	(nM)	% change in B_{max}[a]
CPR	29.4 ± 0.2	20.7 ± 0.2 (***)	+76%
Cytochrome b5	34.4 ± 0.4	16.8 ± 0.3 (***)	+298%

[a] Change in B_{max} for each fitted binding event calculated as percentage in comparison to CYP2C8.1, see Fig. S4 for substrate binding plot.

inhibition was observed for RG, PAC and AQ, inhibition of CER metabolism by cytochrome b5 was less evident. Metabolic activity of CYP2C8.3 for RG, PAC, and AQ remained higher excluding CER metabolism for which CYP2C8.1 and variant demonstrated equal activity.

3.3.2. Effect of CPR

When altering CPR concentrations in the reconstitution system, both wild type and variant showed nonlinear kinetic profiles (Fig. 5). As the DEAQ formation, dependent on CPR, displayed Michaelis–Menten kinetics, apparent $K_{m,red}$ and k_{cat} values were calculated to illustrate the strength of P450 reductase–CYP2C8 complexes. For all substrates, CYP2C8.3 displayed a higher turnover (Fig. 5). Differences in $K_{m,red}$ between CYP2C8.1 and CYP2C8.3 were strongly dependent on the substrate (Table 2). Apparent $K_{m,red}$ values were similar for AQ, CER and RG metabolism for CYP2C8.1, but different for PAC metabolism. Whereas the apparent $K_{m,red}$ did not vary between CYP2C8.1 and CYP2C8.3 for CER metabolism, CYP2C8.3 displayed ~7-times lower $K_{m,red.}$ using PAC 6α-hydroxylation as the probe reaction. CYP2C8.3 showed a similar 2–3 fold decrease of $K_{m,red}$ in comparison to CYP2C8.1 for RG and AQ metabolism. Interestingly, the lowest $K_{m,red.}$ was measured for the molecule with the largest size (PAC), whereas no change in $K_{m,red}$ was measured for the only acidic drug CER.

3.3.3. Reaction uncoupling

NADPH-depletion experiments demonstrated almost no differences in NADPH consumption between CYP2C8.1 and CYP2C8.3 at a ratio CYP2C8:CPR:cytochrome b5 of 1:2:1 ($19.7 \pm 0.1\ min^{-1}$ for CYP2C8.1 during metabolism of AQ or $19.0 \pm 2.4\ min^{-1}$ without substrate, and $23.3 \pm 0.6\ min^{-1}$ for CYP2C8.3 without and

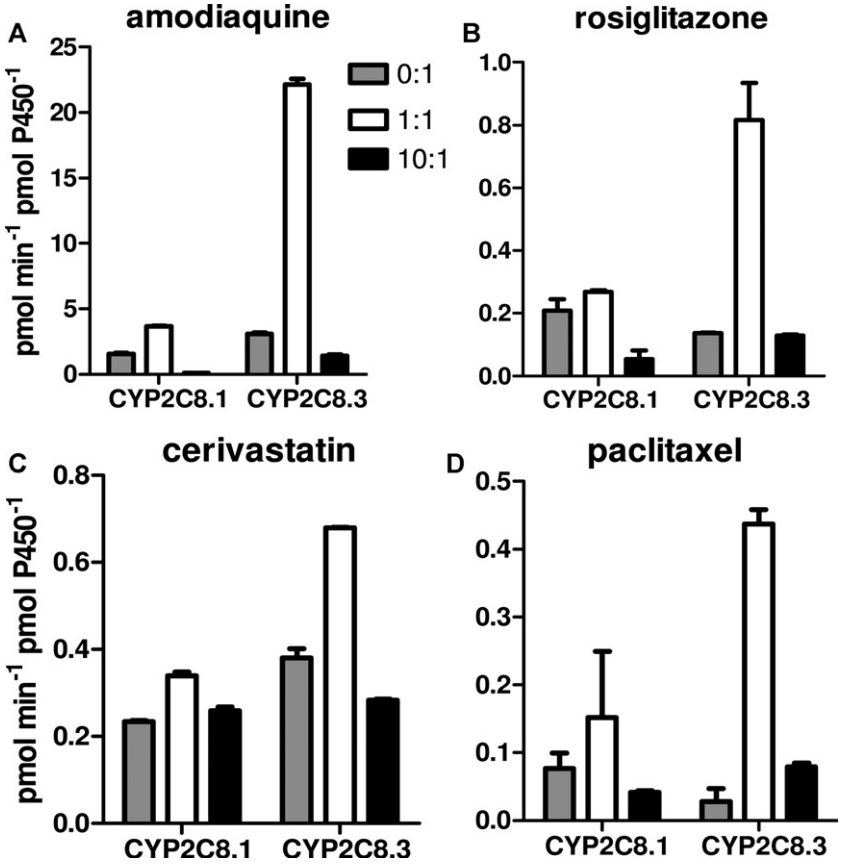

Fig. 4. Reaction rate of AQ *N*-de-ethylation (A), RG *p*-hydroxyation (B), CER hydroxylation (C), PAC 6α-hydroxylation (D) for CYP2C8.1 and CYP2C8.3 proteins measured at different concentrations of cytochrome b5 and constant ratio CYP:CPR 1:1 (for complete kinetic, see Supplementary Information; error bars derived from duplicate measurements).

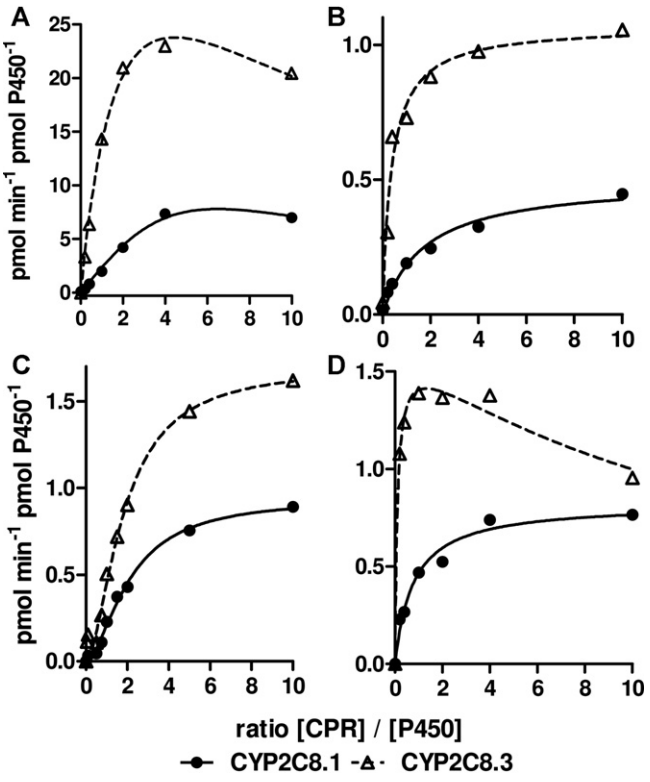

Fig. 5. Reaction rate of (A) AQ *N*-de-ethylation, (B) RG 5-hydroxyation, (C) CER hydroxylation, (D) PAC 6α-hydroxylation measured at different concentrations of CPR and a constant ratio CYP:cytochrome b5 1:1.

18.9 ± 2.2 min^{-1} with AQ). On the other hand, DEAQ formation at an amodiaquine concentration of 5 μM, as mentioned previously, showed a 4-fold increase with CYP2C8.3 protein (Supplementary Data). CYP2C8.1 consumed only 4.3% of depleted NADPH for AQ turnover whereas CYP2C8.3 consumed about four fold higher at 16.9%.

3.4. Structural evaluation, and substrate docking in silico

To test if R139 and K399 are conserved amino acids among various CYP proteins, sequence alignment of CY2C8 with cytochrome P450 enzymes of the CYP2C family, other CYP enzymes related to drug metabolism, and bacterial P450s was performed. R139 was only conserved within the CYP2C sub-family and its closest related drug metabolizing isozymes CYP2B4 and CYP2B6, whereas K399 was only conserved among CYP2C subfamily members and CYP3A4 (Fig. 6). Both residues are positively charged amino acids that differ in size and pK_a (12.1 for Arginine and 10.7 for Lysine). R139 is located next to a positively charged K138 (also conserved within the CYP2 family) with similar physicochemical properties in the flexible hinge region between the C- and D-helix and pointing in the opposite direction. Salt bridges were predicted towards D143 and E147 and disappeared with the R139K mutation in CYP2C8.3 (Fig. 7), elongating the distance from K139 to D143 from 3.4 to 3.9 Å and for K139 to E147 from 2.6 to 3.7 Å in CYP2C8.3. K399 is located in a conserved HDD/NK sequence following the β2 strand and K′-helix and a salt bridge was predicted between R399 and D398 in CYP2C8.3 but not for K399 in CYCP2C8.1. In electrostatic surface calculations, the change in surface charge due to K399R mutation could be visualized as this particular amino acid was oriented outwards, whereas the R139K mutation coordination with the D-helix was almost undetectable (Supplementary Material, S2 and S3).

All four substrates were docked into the active site of CYP2C8 (2NNI). CER, the only acidic substrate used, was found to be bound to S100 in the B′-helix in a productive orientation for oxidation. RG and AQ molecules are both bent over the I-helix not interacting with the B′-helix (data not shown). As previously reported [41], docking of PAC gave an *in silico* K_i in nM range suggesting that the binding model seems unreasonable for this compound (Fig. 8).

3.5. Equilibrium binding studies

The enzyme solution was supplemented with 1% CHAPS to keep the enzyme from aggregating over time and also promote the formation of CYP2C8 monomers [41]. DLPC and glycerol strongly interfered with the spectrometric response. The resting heme iron of CYP2C8.1 was at 5% high spin state with no ligand added whereas for CYP2C8.3, 11% of the heme iron was at high spin after deconvolution of the total spectra (using the program Origin). Binding studies with all four ligands to CYP2C8.1 and CYP2C8.3 revealed two binding phases as was previously shown for retinoic acid [41]. Both phases exhibited a tight ligand binding with K_D values below enzyme concentration, leading to enzyme depletion. The two tight binding modes were not due to an artifact since the

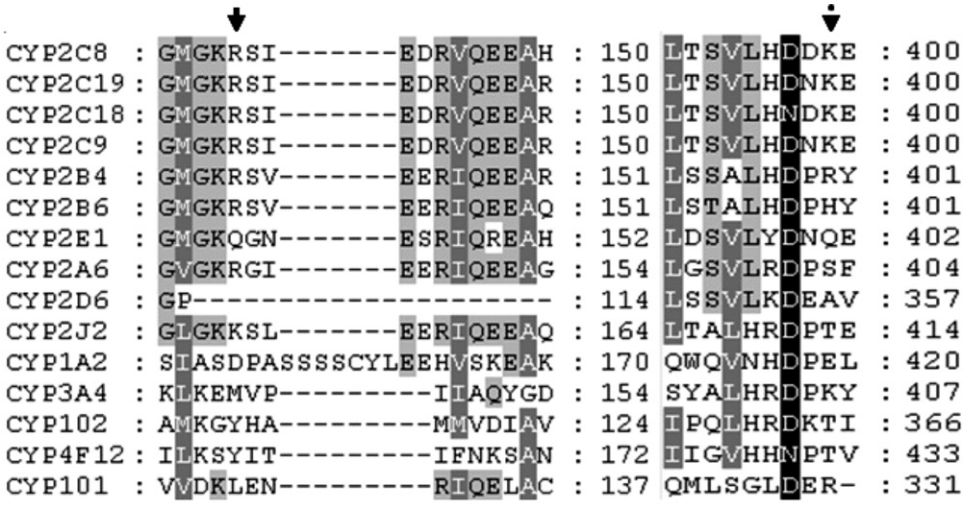

Fig. 6. Sequence alignment of CYP2C8 with the members of its subfamily and other drug metabolizing and bacterial CYP enzymes (for reference sequence see materials and methods, amino acid homology indicated in increasing gray tone).

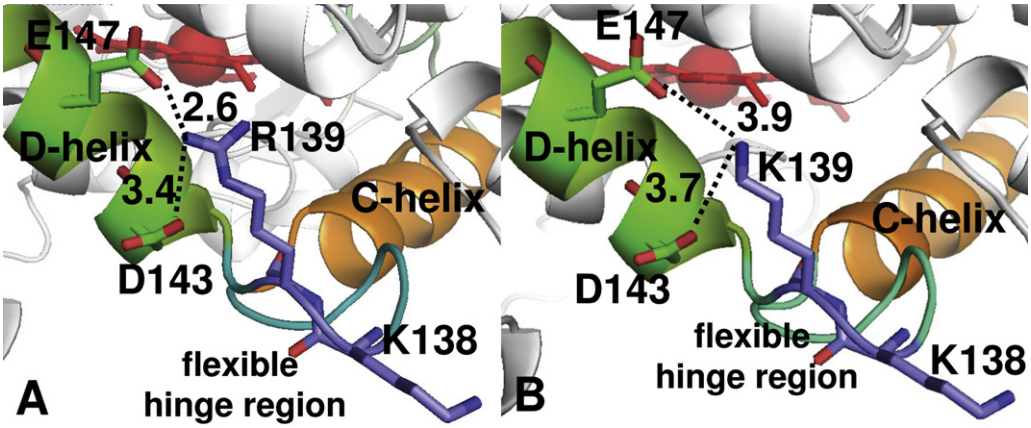

Fig. 7. (A) CYP2C8.1 (2NNI) and (B) CYP2C8.3 (homology model) depicting the impact of the R139K mutation on the distances of the salt bridge network of the hinge region between C and D helices.

results were reproduced with different enzyme concentrations. Fitting the data to a one site binding quadratic equation revealed poor regression analysis (a parameter $n < 1$ as used by Schoch et al. [41]. was calculated, suggesting cooperativity). Consequently, enzyme depletion was neglected and two K_D values were derived from the simpler Michaelis–Menten model for comparative purposes (Supplementary Data Fig. S4). DynaFit calculations with a variable response also indicated a sequential binding model for two substrate molecules binding in the active site as the most suitable fit (in comparison to two independent sites, Hill-equation, one-site and sequential random binding), but values were not significantly different from a Michalis–Menten model and displayed higher deviation.

With the exception of PAC, all substrates had lower K_D values, for the first binding phase, for CYP2C8.3 compared to CYP2C8.1. The K_D for second binding phase also was lower for the CYP2C8.3 variant, except for CER (Table 3). As for PAC and CER, both binding affinities are comparable to the binding of retinoic acid, but AQ and RG displayed a very low initial K_D values initiating a spin state change at <1 nM, which is expected to be inaccurate. The spectroscopic signal amplitude was almost twice as high for CYP2C.3 with all ligands and B_{max} of both binding events similarly increased.

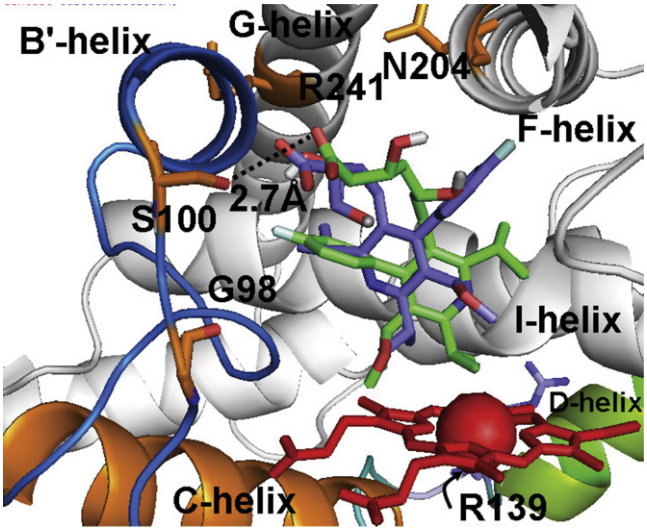

Fig. 8. Active site of CYP2C8 (2NNI) docked with CER in two alternative orientations (representing oxidation at isopropyl group and de-methylation) illustrating the interaction of the acid grouping with the predicted binding region on the B′-helix (G98 and S100) and N204 (F-helix) and R241 (G-helix) (structural features in the foreground removed for simplification).

A spin change of CYP2C8 during binding of redox partners led to a decrease in K_D values for both partners indicating a higher affinity of CPR and cytochrome b5 towards CYP2C8.3 and an up to three times larger induced spectral response for the case of the former.

4. Discussion

This study methodically compares the activity of CYP2C8.1 and its CYP2C8.3 variant using the same expression system and four established CYP2C8 substrates. The variant protein CYP2C8.3, which carries two amino acids changes at R139K and K399R, displays an overall higher *in vitro* activity compared to CYP2C8.1 when reconstituted with cytochrome b5 regardless of substrate (CER, AQ, RG or PAC). This observation contrasts with previous investigations in which recombinant expressed CYP2C8.3 was reported to have a lower activity in comparison to wild type CYP2C8 for PAC and AQ [11,12], but these investigations did not address cytochrome b5 addition or content.

The higher metabolic activity of CYP2C8.3 over CYP2C8.1 seems to be determined predominantly by a higher affinity of CYP2C8.3 to cytochrome b5 (resulting in decreased reaction uncoupling) and CPR, which are both ligand dependent. Amplitude of spin change is particularly strong for cytochrome b5 binding to CYP2C8.3 and the tighter affinity towards cytochrome b5 is suggested to be the dominant contributor to the increased catalytic activity of the variant. Tighter ligand binding, and an overall (up to five fold) larger amplitude of spin change during binding of ligand to CYP2C8.3 in comparison to CYP2C8.1 are suggested to further contribute to an increased catalytic activity.

It is known that cytochrome b5 functions as an activator of P450 mediated drug oxidations, but interestingly enhances the metabolic activity of the variant CYP2C8.3 more strongly than CYP2C8.1. The activation of CYP enzymes by cytochrome b5 is well documented for CYP2C [22,23] and CYP2B sub families [19]. A decrease in P450 reaction uncoupling is proposed to be the main cause of enhanced activity due to cytochrome b5 addition. [23]. Reaction uncoupling itself can vary depending on the substrate metabolized but also on the isozyme studied [44]. Although exact coupling stoichiometry was not assessed for all CYP2C8-substrate pairs here, CYP2C8.3 displayed higher coupling stoichiometry than CYP2C8.1 for DEAQ formation, confirming this hypothesis for the most selective CYP2C8 reaction. However, it seems evident that different amplitudes of activation by cytochrome b5 will depend on substrate used.

Large excess of cytochrome b5 inhibited the metabolic activity for CER, RG and PAC and balanced the metabolic differences between CYP2C8.1 and CYP2C8.3. CYP2C8.1 exhibited a higher

activity for all substrates in absence cytochrome b5 supplementation, which may explain the discrepancy to published reports, as the effect of cytochrome b5 on CYP2C8 catalysis was not investigated previously. This inhibitory effect cannot be generalized, as CYP2C8.3 still exhibited a higher activity for AQ metabolism. Inhibition of product formation by an excess of cytochrome b5 was previously described for CYP2C9 [23] and could be a strong indicator that cytochrome b5 and CPR have an overlapping binding domain and compete for binding to the P450.

In human liver microsomes, a high concentration of cytochrome b5 in comparison to CYP2C8-enzyme may be similarly inhibiting CYP2C8 activity for AQ-metabolism as described above for recombinant CYP2C8, but the effect cannot solely be explained by the cytochrome b5 effect, as the variant was still more active in recombinant enzymes in an excess of cytochrome b5 for AQ. Possibly, other protein interactions in the complex HLM-matrix might influence activity. Higher activity in the *CYP2C8*3* variant was only seen with CYP2C8 for specific substrates such as AQ [45]. Positive correlations were previously found for expressed CYP3A4, 2B6, and 1A2 activity versus the ratio of cytochrome b5 to CYP [43]. For substrates such as RG metabolized by different CYP enzymes (CYP2C9 and CYP3A4) to the *para*-hydroxylated or de-methylated products [46], correlation of CYP2C8 activity with cytochrome b5 content was not apparent likely due to the complexity of the system preventing extrapolation to the actual situation *in vivo* (data not shown). Recent investigations show however, that cytochrome b5 has a major impact on the drug clearance *in vivo* as demonstrated in a hepatic cytochrome b5 null mouse [47,48]. Also, common genetic variants of CPR are reported to affect metabolism of CYP-enzymes [49], and disease related CPR variants can increase CYP2D6 activity two-fold, or abolish activity completely *in vitro* [49,50]. For cytochrome b5, only less common genetic variants are reported [51]. Both cytochrome b5 and CPR content in HLMs decrease with age [52].

On the molecular level, the higher stability of CYP2C8.3-redox partner complex and the receptiveness of the CYP2C8.3 variant towards cytochrome b5 are of particular interest. The amino acid changes R139K and K399R align with the putative overlapping interaction patches of CYP2B4 with cytochrome b5 and CPR in the proximal region to the heme center [16]. As both amino acids are conserved in the CYP2C and CYP2B subfamilies and for interactions with b5, mostly Arginine and Lysines were identified maintaining the charge locally, the possible evolutionary change from Arginine to Lysine and vice versa is remarkable and possibly essential for enzyme activity. As both mutations are genetically tightly linked (linkage disequilibrium >95%), this investigation does not account for the effects of each mutation independently and only rationalizes the separate roles through *in silico* studies.

The mutation R139K results in a reduced pK_a and predicts a weakened hydrogen bond network between the hinge region and D-helix. Several reports support the importance of R139, for example in CYP2B4 an R140A mutation (corresponding to R139 in CYP2C8) was expressed only in an inactive form in *E. coli* in earlier reports, and a neighboring K139A mutation increased the apparent K_D towards CPR by 20-fold [53]. This change could be observed here only modestly in binding studies, but its effect on kinetics in turnover experiments was remarkable as displayed in the lower $K_{m,red}$ for reductase binding to CYP2C8.3 (Table 2).

A possible explanation could be that the compromised salt bridges may destabilize the hinge region between the C and D helices, increase enzyme plasticity and as a result affect the C-helix important for CPR interactions. Cross-linking experiments demonstrated an interaction of CPR, particularly with the corresponding residue R140 in CYP2B4 [54]. Further, a predominant substrate access channel could also be affected as it is suggested to be located between B′ and G-helices [55].

The mutation K399R, exposed from the enzyme surface into solution, seemingly builds a new hydrogen bond and would consequently contribute to a stabilization of the tertiary structure, increase surface charge locally and could consequently affect the affinity for redox partner binding. K399R is reported to contribute more to an increase in k_{cat} and less to the enzymes affinity, but both mutations together seem necessary to maintain activity whereas a single mutation does not display activity at the level of the wild type [64].

Finally, binding affinity of cytochrome b5 and CPR seem to be substrate specific. Investigating substrate binding alone could, at least partially, explain the ability of heme reduction to initiate catalysis in some enzymes such as the closely related CYP2C9 [21] or BM3 [58]. As no direct correlation between amplitude of spin change and k_{cat} is clearly established in general [57], substrate binding could at least have an effect on the subsequent binding of redox partners. Energetically, electron transfer usually correlates with the CYP reduction potential [56] whereas the displacement of water from the active site through ligand binding is indicated by a spin state shift.

The observed increase in K_m values from CYP2C8 wild type to variant for all substrates except CER indicates a decrease in binding affinity for CYP2C8.3. Bulky substrates like PAC might enter the active site, and substrate turnover possibly occurs without complete closure of the P450 and its access channels as suggested by Schoch et al. [41]. A partially open conformation could presumably affect the positioning of the B′-helix encompassing the active site and bend C and D-helices, especially if the salt bridge at K139 is disturbed. This might alter interactions towards CPR and change reactivity depending on substrate fit. $K_{m,red}$ values for PAC were remarkably lower in comparison to the other substrates and illustrate this effect. In contrast, acidic substrates such as CER might stabilize the B′-helix orientation due to a specific interaction with S100 (docking studies), and indicated by a similar $K_{m,red}$ value for CYP2C8.3. S100 is reported to interact particularly with the carboxylate moiety of ligands such retinoic acid, or glucuronides and also with the proximal N204 and R241 of the B′-helix in a second proximal orientation. With an observed two site binding model for all substrates, but single enzyme kinetic model for turnover suggests that the initial induced spin state change might be through a first binding event at a catalytically nonproductive site followed by the second substrate binding in the active site [59,60]. This observation was substantiated by single enzyme kinetics and a very low K_D for AQ and RG in the first binding event. The induction of a spin state shift at such low ligand concentration is particularly exciting, as an allosteric effect could be suggested here. As the calculated K_D values do not align with the K_m values measured for substrate turnover, K_m values might strongly be influenced by the relation of k_{on} to k_{off} rates.

Substrate binding under physiological conditions may differ significantly because high detergent concentration was necessary to generate a CYP2C8 monomer while in solution. CYP2C8 forms at least a dimer [61], and further, other CYP enzymes (or proteins) would certainly interact with CY2C8 in the lipid bilayer of the endoplasmatic reticulum and alter CYP mediated metabolism in liver microsomes e.g. through heterotropic cooperativity. For example, CYP2B4 activity is reported to be lower in presence of CYP1A2 [62]. To date, the actual active (oligomer-)form of a CYP–CPR–b5 complex in liver microsomes is so far unknown and expected to be quite complex [63].

In conclusion, the results of this study demonstrate that cytochrome b5 acts as an activator of CYP2C8, especially CYP2C8.3 for AQ, RG, PAC and CER. *In silico* studies suggest R139 as an essential amino acid influencing CYP–CPR interactions, depending on substrate binding. However, the magnitude of increase in activity could not be translated to the activity in human liver

microsomes, likely due to an inhibitory effect of cytochrome b5. The *in vivo* affect of *CYP2C8*3* will most likely be substrate dependent as well.

Acknowledgement

The authors wish to thank Professor William M. Atkins for his critical evaluation of this manuscript and insightful comments.

Appendix A. Supplementary data

Supplementary data associated with this article can be found, in the online version, at doi:10.1016/j.bcp.2011.06.027.

References

[1] Shimada T, Yamazaki H, Mimura M, Inui Y, Guengerich FP. Interindividual variations in human liver cytochrome P-450 enzymes involved in the oxidation of drugs, carcinogens and toxic chemicals: studies with liver microsomes of 30 Japanese and 30 Caucasians. J Pharmacol Exp Ther 1994;270:414–23.
[2] Rendic S, Di Carlo FJ. Human cytochrome P450 enzymes: a status report summarizing their reactions, substrates, inducers, and inhibitors. Drug Metab Rev 1997;29:413–580.
[3] Totah RA, Rettie AE. Cytochrome P450 2C8: substrates, inhibitors, pharmacogenetics, and clinical relevance. Clin Pharmacol Ther 2005;77:341–52.
[4] Karonen T, Filppula A, Laitila J, Niemi M, Neuvonen PJ, Backman JT. Gemfibrozil markedly increases the plasma concentrations of montelukast: a previously unrecognized role for CYP2C8 in the metabolism of montelukast. Clin Pharmacol Ther 2010;88:223–30.
[5] Kaspera R, Totah RA. Epoxyeicosatrienoic acids: formation, metabolism and potential role in tissue physiology and pathophysiology. Expert Opin Drug Metab Toxicol 2009;5:757–71.
[6] Thatcher JE, Zelter A, Isoherranen N. The relative importance of CYP26A1 in hepatic clearance of all-trans retinoic acid. Biochem Pharmacol 2010;80:903–12.
[7] Dai D, Zeldin DC, Blaisdell JA, Chanas B, Coulter SJ, Ghanayem BI, et al. Polymorphisms in human CYP2C8 decrease metabolism of the anticancer drug paclitaxel and arachidonic acid. Pharmacogenetics 2001;11:597–607.
[8] Kaspera R, Naraharisetti SB, Tamraz B, Sahele T, Cheesman MJ, Kwok P-Y, et al. Cerivastatin in vitro metabolism by CYP2C8 variants found in patients experiencing rhabdomyolysis. Pharmacogen Genom 2010;20:619–29.
[9] Daily EB, Aquilante CL. Cytochrome P450 2C8 pharmacogenetics: a review of clinical studies. Pharmacogenomics 2009;10:1489–510.
[10] Parikh S, Ouedraogo JB, Goldstein JA, Rosenthal PJ, Kroetz DL. Amodiaquine metabolism is impaired by common polymorphisms in CYP2C8: implications for malaria treatment in Africa. Clin Pharmacol Ther 2007;82:197–203.
[11] Gao Y, Liu D, Wang H, Zhu J, Chen C. Functional characterization of five CYP2C8 variants and prediction of CYP2C8 genotype-dependent effects on in vitro and in vivo drug–drug interactions. Xenobiotica 2010;40:467–75.
[12] Soyama A, Hanioka N, Saito Y, Murayama N, Ando M, Ozawa S, et al. Amiodarone N-deethylation by CYP2C8 and its variants, CYP2C8*3 and CYP2C8 P404A. Pharmacol Toxicol 2002;91:174–8.
[13] Smith HE, Jones 3rd JP, Kalhorn TF, Farin FM, Stapleton PL, Davis CL, et al. Role of cytochrome P450 2C8 and 2J2 genotypes in calcineurin inhibitor-induced chronic kidney disease. Pharmacogenet Genomics 2008;18:943–53.
[14] Rowbotham SE, Boddy AV, Redfern CP, Veal GJ, Daly AK. Relevance of non-synonymous CYP2C8 polymorphisms to 13-cis retinoic acid and paclitaxel hydroxylation. Drug Metab Dispos 2010;38:1261–6.
[15] Parikh A, Guengerich FP. Expression, purification, and characterization of a catalytically active human cytochrome P450 1A2:rat NADPH-cytochrome P450 reductase fusion protein. Protein Expr Purif 1997;9:346–54.
[16] Zhang H, Myshkin E, Waskell L. Role of cytochrome b5 in catalysis by cytochrome P450 2B4. Biochem Biophys Res Commun 2005;338:499–506.
[17] Schenkman JB, Jansson I. The many roles of cytochrome b5. Pharmacol Ther 2003;97:139–52.
[18] Guengerich FP, Martin MV, Beaune PH, Kremers P, Wolff T, Waxman DJ. Characterization of rat and human liver microsomal cytochrome P-450 forms involved in nifedipine oxidation, a prototype for genetic polymorphism in oxidative drug metabolism. J Biol Chem 1986;261:5051–60.
[19] Zhang H, Im SC, Waskell L. Cytochrome b5 increases the rate of product formation by cytochrome P450 2B4 and competes with cytochrome P450 reductase for a binding site on cytochrome P450 2B4. J Biol Chem 2007;282:29766–7.
[20] Soucek P. Expression of cytochrome P450 2A6 in *Escherichia coli*: purification, spectral and catalytic characterization, and preparation of polyclonal antibodies. Arch Biochem Biophys 1999;370:190–200.
[21] Locuson CW, Gannett PM, Tracy TS. Heteroactivator effects on the coupling and spin state equilibrium of CYP2C9. Arch Biochem Biophys 2006;449:115–29.
[22] Yamazaki H, Nakamura M, Komatsu T, Ohyama K, Hatanaka N, Asahi S, et al. Roles of NADPH-P450 reductase and apo- and holo-cytochrome b5 on xenobiotic oxidations catalyzed by 12 recombinant human cytochrome P450s expressed in membranes of *Escherichia coli*. Protein Expr Purif 2002;24:329–37.
[23] Locuson CW, Wienkers LC, Jones JP, Tracy TS. CYP2C9 protein interactions with cytochrome b(5): effects on the coupling of catalysis. Drug Metab Dispos 2007;35:1174–81.
[24] Niemi M, Leathart JB, Neuvonen M, Backman JT, Daly AK, Neuvonen PJ. Polymorphism in CYP2C8 is associated with reduced plasma concentrations of repaglinide. Clin Pharmacol Ther 2003;74:380–7.
[25] Porter TD, Wilson TE, Kasper CB. Expression of a functional 78 000 dalton mammalian flavoprotein, NADPH-cytochrome P-450 oxidoreductase, in *Escherichia coli*. Arch Biochem Biophys 1987;254:353–67.
[26] Holmans PL, Shet MS, Martin-Wixtrom CA, Fisher CW, Estabrook RW. The high-level expression in *Escherichia coli* of the membrane-bound form of human and rat cytochrome b5 and studies on their mechanism of function. Arch Biochem Biophys 1994;312:554–65.
[27] Smith PK, Krohn RI, Hermanson GT, Mallia AK, Gartner FH, Provenzano MD, et al. Measurement of protein using bicinchoninic acid. Anal Biochem 1985;150:76–85.
[28] Omura T, Sato R. The carbon monoxide-binding pigment of liver microsomes. I. Evidence for its hemoprotein nature. J Biol Chem 1964;239:2370–8.
[29] Cheesman MJ, Baer BR, Zheng YM, Gillam EM, Rettie AE. Rabbit CYP4B1 engineered for high-level expression in *Escherichia coli*: ligand stabilization and processing of the N-terminus and heme prosthetic group. Arch Biochem Biophys 2003;416:17–24.
[30] Paine MF, Khalighi M, Fisher JM, Shen DD, Kunze KL, Marsh CL, et al. Characterization of interintestinal and intraintestinal variations in human CYP3A-dependent metabolism. J Pharmacol Exp Ther 1997;283:1552–62.
[31] Lowry OH, Rosebrough NJ, Farr AL, Randall RJ. Protein measurement with the Folin phenol reagent. J Biol Chem 1951;193:265–75.
[32] Naraharisetti SB, Lin YS, Rieder MJ, Marciante KD, Psaty BM, Thummel KE, et al. Human liver expression of CYP2C8: gender, age, and genotype effects. Drug Metab Dispos 2010;38:889–93.
[33] Nakano M, Kelly EJ, Rettie AE. Expression and characterization of CYP4V2 as a fatty acid omega-hydroxylase. Drug Metab Dispos 2009;37:2119–22.
[34] Kelley RW, Reed JR, Backes WL. Effects of ionic strength on the functional interactions between CYP2B4 and CYP1A2. Biochemistry 2005;44:2632–41.
[35] Yasukochi Y, Masters BS. Some properties of a detergent-solubilized NADPH-cytochrome c(cytochrome P-450) reductase purified by biospecific affinity chromatography. J Biol Chem 1976;251:5337–44.
[36] Huang W, Lin YS, McConn 2nd DJ, Calamia JC, Totah RA, Isoherranen N, et al. Evidence of significant contribution from CYP3A5 to hepatic drug metabolism. Drug Metab Dispos 2004;32:1434–45.
[37] Bordoli L, Kiefer F, Arnold K, Benkert P, Battey J, Schwede T. Protein structure homology modeling using SWISS-MODEL workspace. Nat Protoc 2009;4:1–13.
[38] Baker NA, Sept D, Joseph S, Holst MJ, McCammon JA. Electrostatics of nanosystems: application to microtubules and the ribosome. Proc Natl Acad Sci U S A 2001;98:10037–41.
[39] Humphrey W, Dalke A, Schulten K. VMD: visual molecular dynamics. J Mol Graph 1996;14(33-8):27–8.
[40] Kuzmic P. Program DYNAFIT for the analysis of enzyme kinetic data: application to HIV proteinase. Anal Biochem 1996;237:260–73.
[41] Schoch GA, Yano JK, Sansen S, Dansette PM, Stout CD, Johnson EF. Determinants of cytochrome P450 2C8 substrate binding structures of complexes with montelukast, troglitazone, felodipine, and 9-cis-retinoic acid. J Biol Chem 2008;283:17227–3.
[42] Lin YS, Dowling AL, Quigley SD, Farin FM, Zhang J, Lamba J, et al. Co-regulation of CYP3A4 and CYP3A5 and contribution to hepatic and intestinal midazolam metabolism. Mol Pharmacol 2002;62:162–72.
[43] Venkatakrishnan K, von Moltke LL, Court MH, Harmatz JS, Crespi CL, Greenblatt DJ. Comparison between cytochrome P450 (CYP) content and relative activity approaches to scaling from cDNA-expressed CYPs to human liver microsomes: ratios of accessory proteins as sources of discrepancies between the approaches. Drug Metab Dispos 2000;28:1493–504.
[44] Cryle MJ, De Voss JJ. The role of the conserved threonine in P450 BM3 oxygen activation: substrate-determined hydroxylation activity of the Thr268Ala mutant. Chembiochem 2008;9:261–6.
[45] Walsky RL, Obach RS. Validated assays for human cytochrome P450 activities. Drug Metab Dispos 2004;32:647–60.
[46] Baldwin SJ, Clarke SE, Chenery RJ. Characterization of the cytochrome P450 enzymes involved in the in vitro metabolism of rosiglitazone. Br J Clin Pharmacol 1999;48:424–32.
[47] McLaughlin LA, Ronseaux S, Finn RD, Henderson CJ, Roland Wolf C. Deletion of microsomal cytochrome b5 profoundly affects hepatic and extrahepatic drug metabolism. Mol Pharmacol 2010;78:269–78.
[48] Finn RD, McLaughlin LA, Ronseaux S, Rosewell I, Houston JB, Henderson CJ, et al. Defining the in Vivo Role for cytochrome b5 in cytochrome P450 function through the conditional hepatic deletion of microsomal cytochrome b5. J Biol Chem 2008;283:31385–93.
[49] Sandee D, Morrissey K, Agrawal V, Tam HK, Kramer MA, Tracy TS, et al. Effects of genetic variants of human P450 oxidoreductase on catalysis by CYP2D6 in vitro. Pharmacogenet Genomics 2010;20:677–86.

[50] Agrawal V, Huang N, Miller WL. Pharmacogenetics of P450 oxidoreductase: effect of sequence variants on activities of CYP1A2 and CYP2C19. Pharmacogenet Genomics 2008;18:569–76.
[51] Kurian JR, Longlais BJ, Trepanier LA. Discovery and characterization of a cytochrome b5 variant in humans with impaired hydroxylamine reduction capacity. Pharmacogenet Genomics 2007;17:597–603.
[52] Gan L, von Moltke LL, Trepanier LA, Harmatz JS, Greenblatt DJ, Court MH. Role of NADPH-cytochrome P450 reductase and cytochrome-b5/NADH-b5 reductase in variability of CYP3A activity in human liver microsomes. Drug Metab Dispos 2009;37:90–6.
[53] Bridges A, Gruenke L, Chang YT, Vakser IA, Loew G, Waskell L. Identification of the binding site on cytochrome P450 2B4 for cytochrome b5 and cytochrome P450 reductase. J Biol Chem 1998;273:17036–49.
[54] Bumpus NN, Hollenberg PF. Cross-linking of human cytochrome P450 2B6 to NADPH-cytochrome P450 reductase: identification of a potential site of interaction. J Inorg Biochem 2010;104:485–8.
[55] Fishelovitch D, Shaik S, Wolfson HJ, Nussinov R. Theoretical characterization of substrate access/exit channels in the human cytochrome P450 3A4 enzyme: involvement of phenylalanine residues in the gating mechanism. J Phys Chem B 2009;113:13018–25.
[56] Ost TW, Clark J, Mowat CG, Miles CS, Walkinshaw MD, Reid GA, et al. Oxygen activation and electron transfer in flavocytochrome P450 BM3. J Am Chem Soc 2003;125:15010–2.
[57] Guengerich FP, Johnson WW. Kinetics of ferric cytochrome P450 reduction by NADPH-cytochrome P450 reductase: rapid reduction in the absence of substrate and variations among cytochrome P450 systems. Biochemistry 1997;36:14741–50.
[58] Noble MA, Miles CS, Chapman SK, Lysek DA, MacKay AC, Reid GA, et al. Roles of key active-site residues in flavocytochrome P450 BM3. Biochem J 1999;339(Pt 2):371–9.
[59] Davydov DR, Halpert JR. Allosteric P450 mechanisms: multiple binding sites, multiple conformers or both? Expert Opin Drug Metab Toxicol 2008;4:1523–35.
[60] Atkins WM. Current views on the fundamental mechanisms of cytochrome P450 allosterism. Expert Opin Drug Metab Toxicol 2006;2:573–9.
[61] Hu G, Johnson EF, Kemper B. CYP2C8 exists as a dimer in natural membranes. Drug Metab Dispos 2010;38:1976–83.
[62] Backes WL, Batie CJ, Cawley GF. Interactions among P450 enzymes when combined in reconstituted systems: formation of a 2B4–1A2 complex with a high affinity for NADPH-cytochrome P450 reductase. Biochemistry 1998;37:12852–9.
[63] Backes WL, Kelley RW. Organization of multiple cytochrome P450s with NADPH-cytochrome P450 reductase in membranes. Pharmacol Ther 2003;98:221–33.
[64] Soyama A, Saito Y, Hanioka N, Murayama N, Nakajima O, Katori N, et al. Non-synonymous single nucleotide alterations found in the CYP2C8 gene result in reduced in vitro paclitaxel metabolism. Biol Pharm Bull 2001;24:1427–30.